Proceedings of the ASME 2022 41st International Conference on Ocean, Offshore and Arctic Engineering OMAE2022
June 5-10, 2022, Hamburg, Germany

OMAE2022-79081

A THREE DEGREES OF FREEDOM VIBRATION MODEL FOR A PARTIALLY INSTALLED WIND TURBINE

Andreas F. Haselsteiner *
University of Bremen
Bremen, Germany
Email: a.haselsteiner@uni-bremen.de

Aljoscha Sander
University of Bremen
Bremen, Germany
Email: alsander@uni-bremen.de

Klaus-Dieter Thoben
University of Bremen
Bremen, Germany
Email: thoben@uni-bremen.de

ABSTRACT

Most offshore wind turbines are installed using the so-called single blade installation procedure. This means that after the tower, nacelle, and hub are installed, the rotor blades are mounted individually. This process step is difficult and sometimes leads to delays because relative motions between the hub and rotor blade need to be small and predictable to enable the successful mounting of the blade. Previously published measurements showed that the tower vibrates in a motion where the nacelle moves in "orbits" that often change shape and axis direction. In this work, we present a simple vibration model that captures some characteristics of the tower dynamics. The model represents the tower and the nacelle as two planar rigid bodies that are connected with a torsional spring. It has three degrees of freedom: the first body's motion in x- and y-direction and the second body's rotation around the first body. An offset between the second body's center of mass and its point of rotation couples the translation of the first body with the rotation of the second body. For some configurations of the parameters that describe mass distribution, stiffness, and geometry, the model produces motion similar to wind turbines during installation: orbits that change in shape and direction. These complex motions occur even without external forcing. For other configurations, however, the tower vibrates in a stationary orbit.

1 Introduction

The designs and industrial processes of offshore wind turbines have improved steadily over the last decade. These improvements enabled bottom-fixed offshore wind turbines to produce electricity at a price that can compete with coal and nuclear energy. Nevertheless, the expansion of offshore wind energy requires further enhancements of designs and processes.

A brief but challenging phase in the lifetime of an offshore wind turbine is its installation (a recent review on turbine installation is provided by Jiang [1]). Currently, most turbines are installed by assembling the main components at the offshore site using an installation vessel. While different procedures such as lifting the completely preassembled rotor have been used in the past [2], typically, each rotor blade is installed individually offshore now. This so-called "single blade installation" procedure is difficult [3, 4, 5] and sometimes leads to delays because motions between hub and rotor blade need to be small and predictable to enable the successful mounting of the blade.

Previously published measurements [6, 7] showed that before the blades were installed, the partially installed turbine vibrated in a motion where the nacelle moved in "orbits" that often changed shape and axis direction (Figure 1). These motions were significant in magnitude and appeared somewhat erratic. They likely caused delays in previous wind farm installations. As new turbine designs become greater in size, they are expected to become more flexible such that vibrations could become even more severe. At the moment, the dynamics of these motions are not well understood. If models to predict vibrations of partially installed wind turbines were available, engineers could use them to design structures that vibrate in a manner that is more favorable to installation procedures. Additionally, installation procedures could be adapted based on a better understanding of the expected vibrations.

*Address all correspondence to this author.

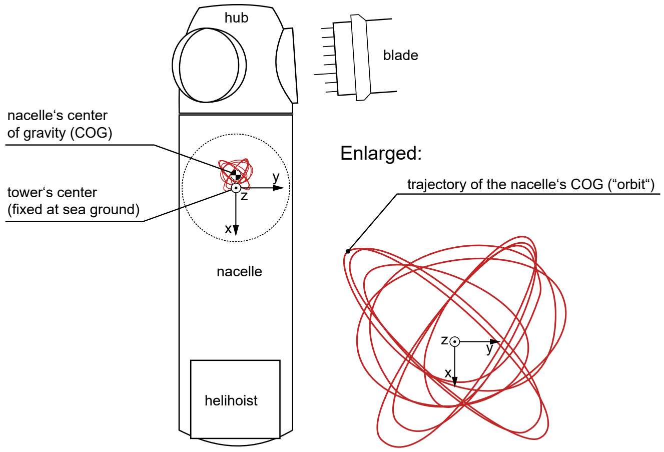

FIGURE 1. Formation of orbits as observed during the installation of the offshore wind farm "Trianel Windpark Borkum II." Note: to enhance visibility, the orbits are not to scale.

While models can have various forms, in this work, our aim was the description of a simple mechanical system that captures the most important characteristics of the observed vibration behavior. Such an approach is common in the study of vibrations: One aims to describe the real system with the simplest model that captures the main dynamics of the real system. Many vibration phenomena can be sufficiently described with systems with only one or two degrees of freedom (see, for example, [8]). Here, we present a model with three degrees of freedom that captures important characteristics of the real system, a partially installed offshore wind turbine.

This work builds on a preprint that was published in 2021 [9]. It presents a simple vibration model for wind turbines in the "hammerhead configuration" (tower and nacelle installed, but no blades yet). The model represents the tower and the nacelle as two planar rigid bodies that are connected with a torsional spring. It has three degrees of freedom: the first body's motion in x- and y-direction and the second body's rotation around the first body. Thus, its dynamics can be described with three equations of motion. The next chapter will present the mathematics of this vibration model. Then, Chapter 3 will present results for some parameter values that represent a simple tabletop experiment and an offshore wind turbine. Finally, Chapter 4 will provide a discussion and conclusions.

2 Vibration model

We model the real system in two dimensions (Figure 2). The tower's bending is modeled as a linear spring, which is connected to a fixed point that represents the turbine's foundation, and to a first body that represents the tower's top section. The tower's torsion is modeled with a torsional spring that connects a second body with a fixed angle in the inertial reference frame. This second body is pinned to the first body such that it translates with the first body, but rotates freely. Consequently, the system's three degrees of freedom are the first body's position in x and y direction and the second body's orientation θ.

Importantly, the second body's center of mass has an offset from its center of rotation such that it acts as an eccentric mass. This offset d causes coupling between the translation of the first body and the rotation of the second body.

By applying the physical laws of conservation of linear and angular momentum, we derived the equations of motions for the system (a derivation is presented in an online repository). The system's equations of motion read:

$$(m_1+m_2)\ddot{x}-\cos(\theta)m_2d\ddot{\theta}+\sin(\theta)m_2d\dot{\theta}^2+k_1x=0, \quad (1)$$

$$(m_1+m_2)\ddot{y}-\sin(\theta)m_2d\ddot{\theta}-\cos(\theta)m_2d\dot{\theta}^2+k_1y=0, \quad (2)$$

$$(I_{zz}+m_2d^2)\ddot{\theta}-\cos(\theta)m_2d\ddot{x}-\sin(\theta)m_2d\ddot{y}+k_2\theta=0, \quad (3)$$

where m_1 and m_2 are the masses of the two bodies, I_{zz} is the second body's moment of inertia, d is the distance between them, k_1 is the stiffness of the spring that connects the first body with the origin, k_2 is the torsional stiffness of the spring between the first and second body, x and y denote the position of the first body's center and θ denotes the orientation of the second body (Figure 2). Dots are used to denote time derivatives.

The equations can be arranged to have only acceleration on the left hand side:

$$\ddot{x}=\frac{1}{m_1+m_2}\left[\cos(\theta)m_2d\ddot{\theta}-\sin(\theta)m_2d\dot{\theta}^2-k_1x\right], \quad (4)$$

$$\ddot{y}=\frac{1}{m_1+m_2}\left[\sin(\theta)m_2d\ddot{\theta}+\cos(\theta)m_2d\dot{\theta}^2-k_1y\right], \quad (5)$$

$$\ddot{\theta}=\frac{1}{I_{zz}+m_2d^2}\left[(\cos(\theta)m_2d\ddot{x}+\sin(\theta)m_2d\ddot{y}-k_2\theta\right]. \quad (6)$$

Several terms couple translation (x and y) with rotation (θ): for example, the acceleration in the x direction, $\ddot{x}$, is equal to terms that contain $\dot{\theta}$ and $\ddot{\theta}$ (Equation 4). Such coupling terms are necessary to appear in the equation as otherwise orbits would not

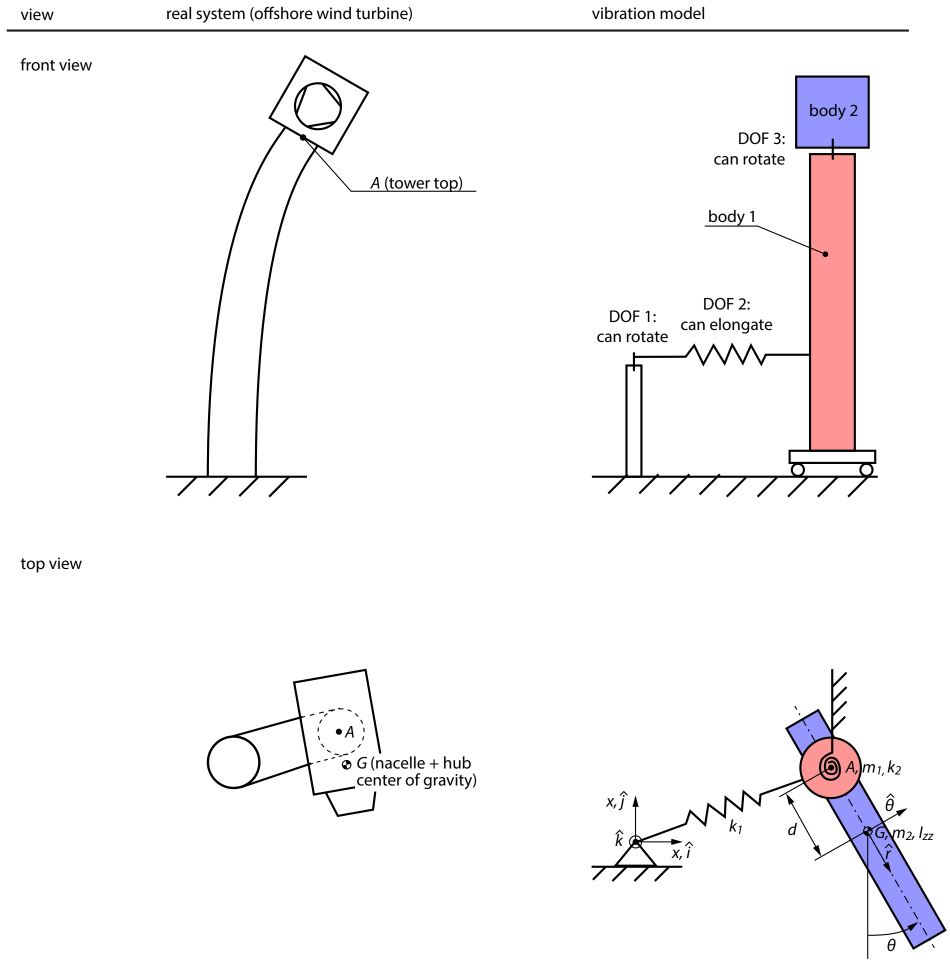

FIGURE 2. The proposed vibration model consists of two discrete bodies and has three degrees of freedom (DOF). Due to the offset d, the second body acts as an eccentric mass. This eccentricity leads to coupling between the translation of body 1 and the rotation of body 2.

change direction (for example, a mass that is initially displaced would indefinitely move in a straight line or a mass that is in an initial orbit would stay in it indefinitely).

The translational acceleration ($\ddot{x}$ and $\ddot{y}$ in Equations 4 and 5) is affected by the second mass' centrifugal and Euler forces. Centrifugal force acts in the $-\hat{r}$ direction (a coordinate system is shown in Figure 2) and reads,

$$m_2 d\dot{\theta}^2, \tag{7}$$

and Euler force acts in the $\hat{\theta}$ direction and reads

$$m_2 d\ddot{\theta}. \tag{8}$$

The equation for $\ddot{\theta}$ (Equation 6) was derived by applying conservation of angular momentum around the second body's center of mass G. The force that acts at the location where the second body is pinned to the first body (point A in Figure 2) depends on the first body's acceleration in x and y direction such that there are also coupling terms with $\ddot{x}$ and $\ddot{y}$ in the equation for $\ddot{\theta}$.

As expected, the equations also show that if $d = 0$ the coupling terms disappear:

$$(m_1 + m_2)\ddot{x} = -k_1 x, \tag{9}$$

$$(m_1 + m_2)\ddot{y} = -k_1 y, \tag{10}$$

$$I_{zz}\ddot{\theta} = -k_2 \theta. \tag{11}$$

3 Dynamics for different system configurations

To understand the dynamic behavior of the model, we analyzed its motion for three configurations (each with different values for the two masses, the moment of inertia, the distance between the two masses, and the stiffness of the two springs):

- a configuration that can be realized as a simple tabletop experiment (results of this experiment were presented in reference [9]; the "tower top" moved in orbits that changed their direction);
- a configuration that we consider to represent a modern wind turbine (the appendix provides details); and
- an unfavorable wind turbine configuration where torsional stiffness is lower and the nacelle's center of mass is farther away from the foundation's center (in this configuration bending and torsion eigenfrequency are in close proximity).

The parameter values of the three configurations are listed in Table 1. Note that compared to [9], in this paper, the parameter values in configurations 2 and 3 were changed to better represent wind turbines.

With parameter values similar to the tabletop experiment, the vibration model leads to similar motions: orbits with changing main axis directions appear (Figure 3). With parameters values that we consider similar to a typical modern offshore wind turbine in the hammerhead configuration, orbit direction changes do not occur. If the torsional stiffness is very high such that torsional motions are very low, the orbit is stable (Figure 4; we consider this scenario typical for a modern wind turbine). In an unfavorable wind turbine configuration with low torsional stiffness orbits that change direction appear (Figure 5).

4 Discussion and conclusions

The vibration model presented in this paper leads to orbits comparable to a tabletop experiment presented in previous work [9] if the parameters of the differential equations are chosen, such that they are close to the parameters of the tabletop experiment. However, for parameters resembling a typical offshore wind turbine, orbits were stable and hardly changed direction. When the torsional stiffness was reduced, orbits became unstable again (they changed direction). This should be investigated further in the future. It would be interesting to investigate whether a clear boundary between parameter value combinations that lead to stable dynamics and combinations that lead to unstable dynamics exist. And if such a boundary – a bifurcation in the parameter space – exists, it would be interesting to investigate its topology.

In summary, the model presented here succeeded in describing some of the characteristics that we observed in vibrating wind turbines in the hammerhead configuration and in a simple tabletop experiment: orbits that change direction. In the vibration model these changing directions are not caused by external forces but by characteristics of the structure: The nacelle's mass, which has an offset relative to the tower's center, causes coupling between torsional and translational motions. However, for parameter values that we consider typical for offshore wind turbines, the coupling was negligible. Only in an unfavorable configuration with artificially low torsional stiffness, strong coupling was present.

Future research could try to better understand under which configurations (masses, stiffness, offsets, ...) the system behaves in which manner. Possibly, classes of motion can be differentiated if there are systems that are "dynamically stable" while others are unstable. Future applications of the presented model could lie in the design process of wind turbines and in the improvement of installation processes.

Appendix: Parameter values to model an offshore wind turbine

The following parameter values were assumed to represent a typical offshore wind turbine with about 6 MW. Some values were losely based on the Senvion turbine 6M152, for which vibration measurements are available [6, 7], while others are based on back-of-the-envelope calculations:

- **mass m_1:** 800×10^3 kg (monopile part that is above the mudline and transition piece + 80 m tower; 500 tons + 300 tons; a discussion on the substructure of a 6 MW turbine is provided by [10]).
- **mass m_2:** 400×10^3 kg (nacelle-hub assembly of a 6 MW turbine).
- **stiffness k_1:** $400 \times 10^3\,\mathrm{N\,m^{-1}}$. The value was chosen such that the eigenperiod is 3 s; $M = m_1 + m_2; T = 3\,\mathrm{s}; k_1 = M \times (2\pi/T)^2$.
- **stiffness k_2:** Calculated by assuming that the tower and monopile torsion behaves like a steel tube with constant diameter and a constant wall thickness. Tube radius $r = 6\,\mathrm{m}$, wall thickness $t = 2.3\,\mathrm{cm}$, $I_T = 2\pi r^3 t$. $k_2 = G_{steel} I_T / h$ with $G_{steel} = 80 \times 10^9$, height $h = 100\,\mathrm{m}$.
- **distance d:** 0.3 m (estimated distance between the hub-nacelle assembly's center of gravity and the tower top's center for a 6 MW turbine; this offset is intended because when the tower of an operating wind turbine bends due to wind loads, the hub-nacelle's weight is closer to the foundation's center).
- **moment of inertia I_{zz}:** $4 \times 10^7\,\mathrm{kg\,m^2}$ (estimated nacelle-hub assembly's moment of inertia around the vertical axis for a 6 MW turbine)

These parameters correspond to a bending eigenfrequency of 0.32 Hz and a torsional eigenfrequency of 1.38 Hz ($f_{0,bending} = 1/(2\pi)\sqrt{k_1/(m_1+m_2)}$, $f_{0,torsion} = 1/(2\pi)\sqrt{k_2/(I_{zz}+m_2 d^2)}$). The order of magnitude compares well with other studies: Bir and Jonkman (2008) [11] found a bending eigenfrequency of

Quantity	Tabletop experiment (results are presented in [9])	Offshore turbine (Typical configuration*)	Offshore turbine (Unfavorable configuration)	Unit
m_1	0.0093	800×10^3	800×10^3	kg
m_2	0.044	400×10^3	400×10^3	kg
k_1	4.5	5×10^6	5×10^6	$\mathrm{N\,m^{-1}}$
k_2	0.057	3×10^9	2×10^8	$\mathrm{Nm\,rad^{-1}}$
d	0.038	0.3	1.0	m
I_{zz}	5×10^{-5}	4×10^7	4×10^7	$\mathrm{kg\,m^2}$
Resulting bending eigenf.	1.46	0.32	0.32	$\mathrm{s^{-1}}$
Resulting torsion eigenf.	3.57	1.38	0.35	$\mathrm{s^{-1}}$
Initial condition				
$x(t=0)$	0.1	1	1	m
$y(t=0)$	0.1	1	1	m
$\dot{x}(t=0)$	0	1	1	$\mathrm{m\,s^{-1}}$
$\dot{y}(t=0)$	0	0	0	$\mathrm{m\,s^{-1}}$

TABLE 1. Values used in the vibration model that roughly correspond to a tabletop experiment [9] and measurements of partially installed offshore wind turbines [6,7]. The resulting kinematics are presented in Figures 3, 4, and 5. The resulting bending eigenfrequency was calculated as $f_{0,bending} = 1/(2\pi)\sqrt{k_1/(m_1+m_2)}$ and the resulting torsion eigenfrequency as $f_{0,torsion} = 1/(2\pi)\sqrt{k_2/(I_{zz}+m_2 d^2)}$. *A derivation of these parameter values is provided in the appendix.

0.25 Hz and a torsion eigenfrequeny of 1.27 Hz for a 5 MW turbine supported on a monopile. Similar values for the 5 MW turbine were found by Chaves Júnior et al. (2020) [12].

Data availablilty

Software to numerically solve the presented equations of motions is available on Github: `https://github.com/ahaselsteiner/2022-vibration-model`. The repository also contains a derivation of the vibration model's equations of motion.

Acknowledgements

AFH thanks J. Kim Vandiver for his excellent lectures on engineering mechanics and MIT for making videos of them publicly available.

REFERENCES

[1] Jiang, Z., 2021. "Installation of offshore wind turbines: A technical review". *Renewable and Sustainable Energy Reviews,* ***139***, p. 110576.

[2] Ahn, D., Shin, S. C., Kim, S. Y., Kharoufi, H., and Kim, H. C., 2017. "Comparative evaluation of different offshore wind turbine installation vessels for Korean west–south wind farm". *International Journal of Naval Architecture and Ocean Engineering,* ***9***, pp. 45–54.

[3] Verma, A. S., Jiang, Z., Vedvik, N. P., Gao, Z., and Ren, Z., 2019. "Impact assessment of a wind turbine blade root during an offshore mating process". *Engineering Structures,* ***180***, pp. 205–222.

[4] Verma, A. S., Jiang, Z., Ren, Z., Gao, Z., and Vedvik, N. P., 2019. "Response-based assessment of operational limits for mating blades on monopile-type offshore wind turbines". *Energies,* ***12***(10), pp. 1–26.

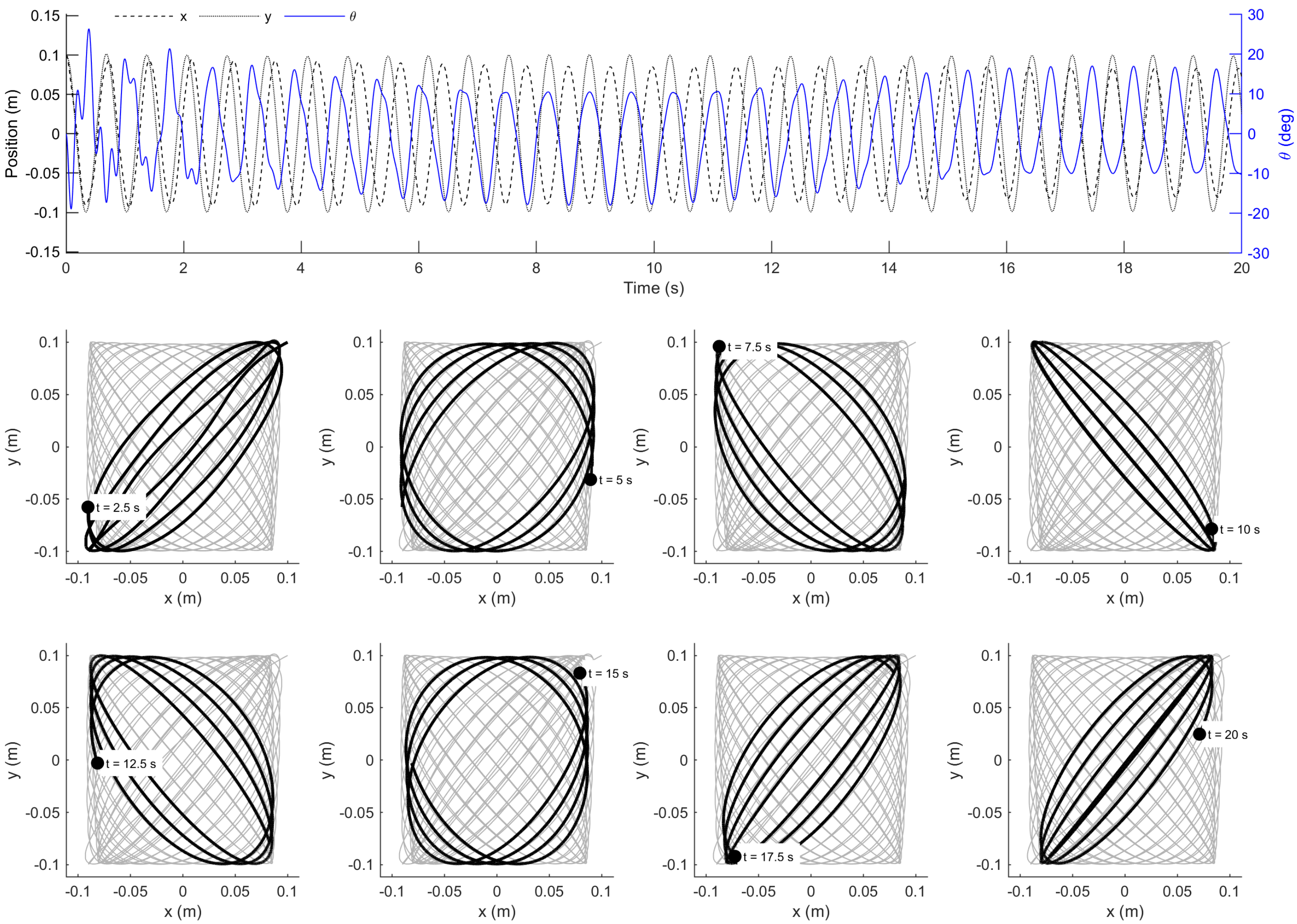

FIGURE 3. Kinematics of the vibration model in the tabletop configuration (Table 1).

[5] Ren, Z., Skjetne, R., Jiang, Z., Gao, Z., and Verma, A. S., 2019. "Integrated GNSS/IMU hub motion estimator for offshore wind turbine blade installation". *Mechanical Systems and Signal Processing,* ***123***, pp. 222–243.

[6] Sander, A., Haselsteiner, A. F., Barat, K., Janssen, M., Oelker, S., Ohlendorf, J.-H., and Thoben, K.-D., 2020. "Relative motion during single blade installation: Measurements from the North Sea". In Proc. 39th International Conference on Ocean, Offshore and Arctic Engineering (OMAE 2020), American Society of Mechanical Engineers (ASME).

[7] Sander, A. Oscillations of Offshore Wind Turbines undergoing Installation I: Raw Measurements.

[8] Naess, A., and Moan, T., 2013. *Stochastic dynamics of marine structures*. Cambridge University Press, Cambridge, United Kingdom.

[9] Sander, A., Haselsteiner, A., and Holman, B., 2021. "Could mass eccentricity explain the formation of orbits in wind turbines?".

[10] Seidel, M., 2012. "6MW turbines with 150 m+ rotor diameter - What is the impact on substructures?". *Proceedings of DEWEK 2012 Bremen, Germany*.

[11] Bir, G., and Jonkman, J., 2008. "Modal dynamics of large wind turbines with different support structures". In Proc. 27th International Conference on Offshore Mechanics and Arctic Engineering (OMAE 2008), American Society of Mechanical Engineerings (ASME).

[12] Chaves Júnior, C. V., Araújo, R. C. d. A., de Souza, C. M. C., Ferreira, A. C. A., and Ribeiro, P. M. V., 2020. "A collocation method for bending, torsional and axial vibrations of offshore wind turbines on monopile foundations". *Ocean Engineering,* ***217***.

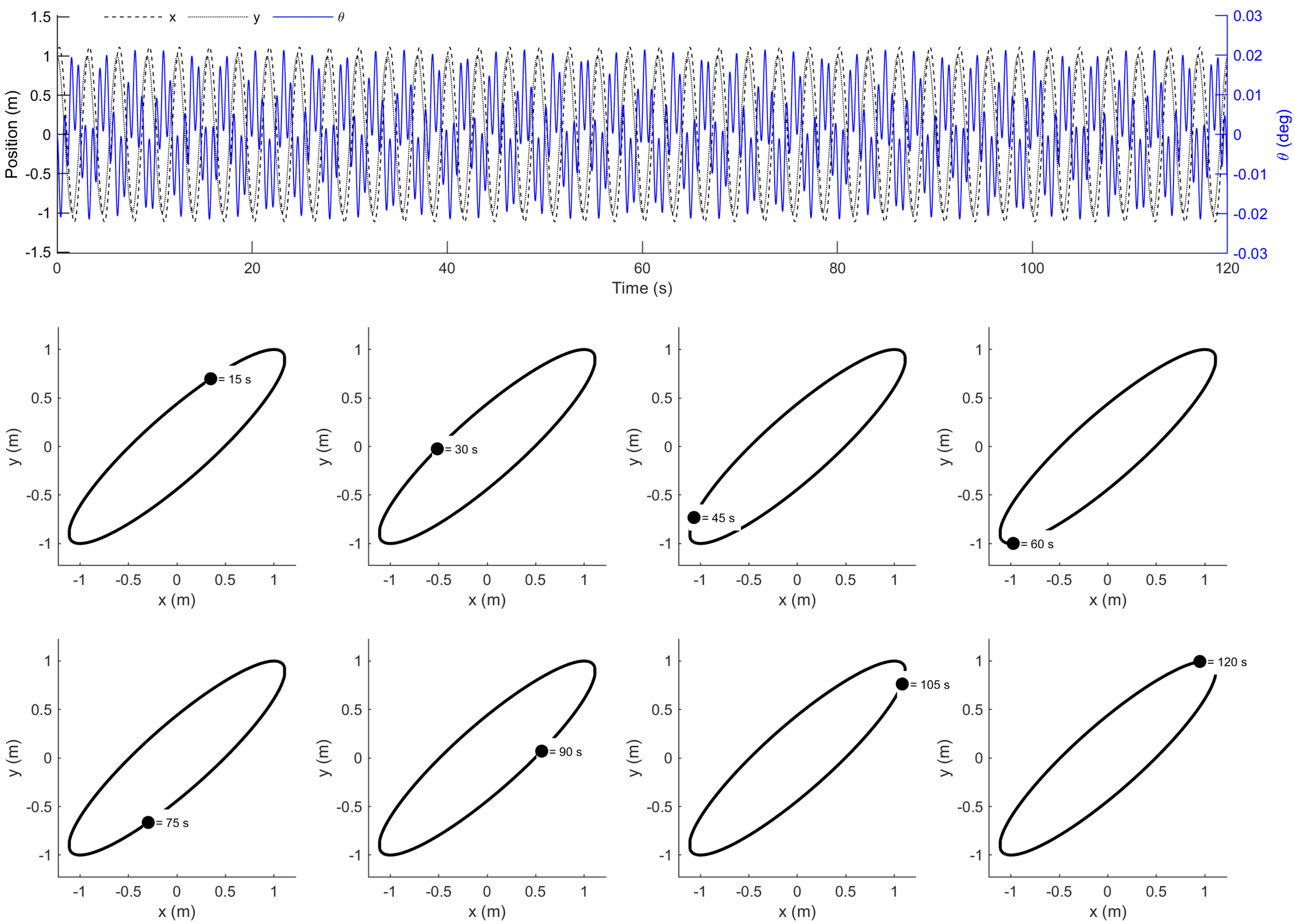

FIGURE 4. Kinematics of the vibration model in a typical wind turbine configuration (Table 1).

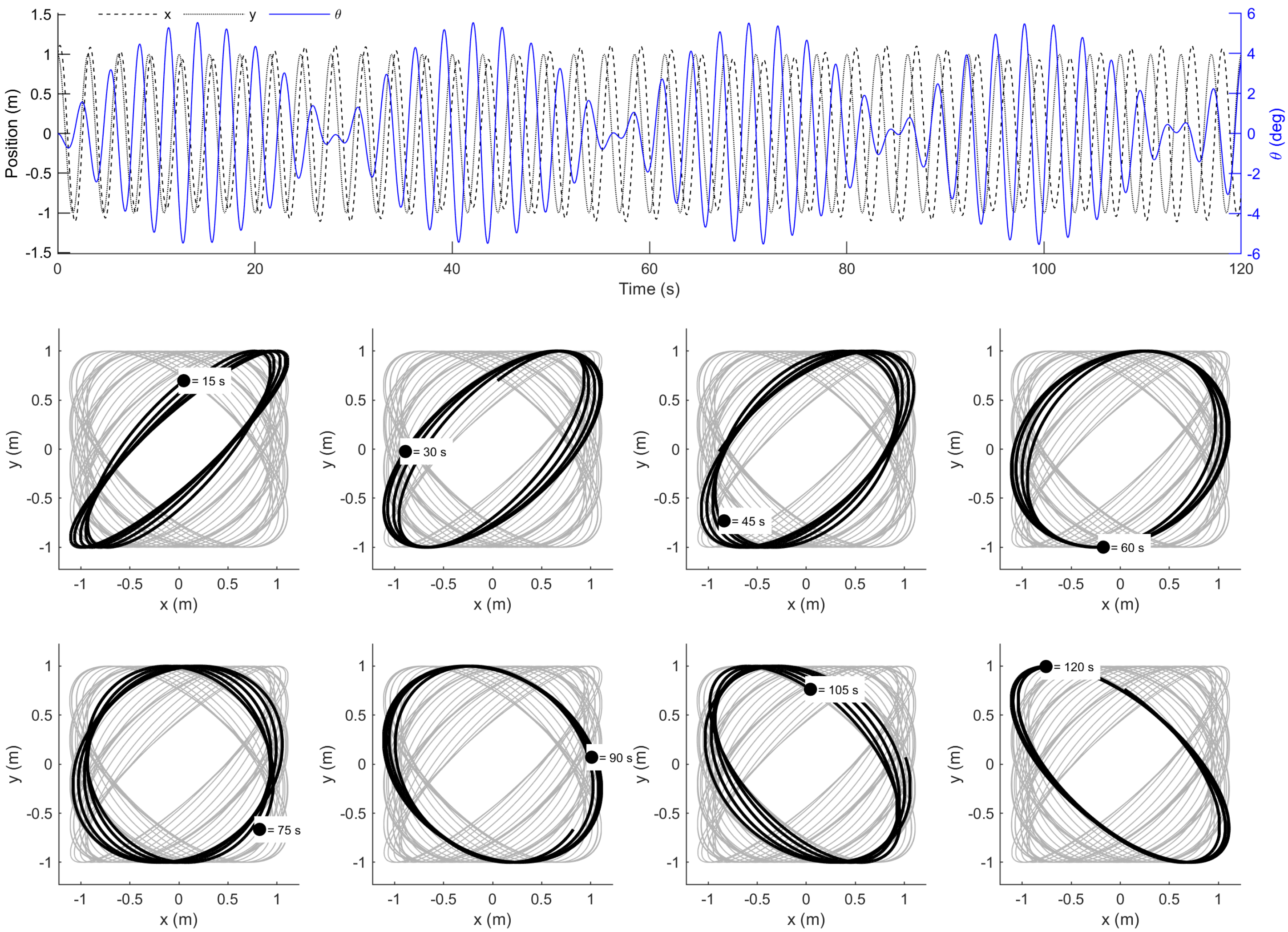

FIGURE 5. Kinematics of the vibration model in an unfavorable wind turbine configuration (Table 1). Parameters values were chosen such that bending and torsion eigenfrequency are close to each other.